Fachtagung "Lasermethoden in der Strömungsmesstechnik"
7. – 9. September 2010, Cottbus

ÜBER DIE VERANTWORTLICHE MECHANISMUS FÜR TURBULENTEN REIBUNGSVERMINDERUNG DURCH ZUGABE VON VERDÜNNTER HOCHPOLYMEREN: THEORIE UNTERSTÜTZT DURCH LDA MESSUNGEN

ON THE MECHANISM RESPONSIBLE FOR TURBULENT DRAG REDUCTION BY DILUTE ADDITION OF HIGH POLYMERS: THEORY SUPPORTED BY LDA MEASUREMENTS

J. Jovanović[1,2], B. Frohnapfel[1,2], B. Z. Genç[1,3], A. Delgado[1,3]
[1]) Lehrstuhl für Strömungsmechanik, Friedrich-Alexander-Universität Erlangen-Nürnberg,
Cauerstr. 4, D-91058 Erlangen
[2]) Center for Smart Interfaces, Technische Universität Darmstadt, Petersenstr. 32, D-64287 Darmstadt
[3]) Erlangen Graduate School of Advanced Optical Technologies (SAOT),
Paul-Gordan-Str. 6, D-91052 Erlangen

Schlagworte: Reibungsverminderung durch Polymere, Laser-Doppler Anemometrie, Brechungsindexanpassung
Keywords: Polymer Drag Reduction, Laser-Doppler Anemometry, Refractive Index Matching

Abstract

Turbulent drag reduction by dilute addition of high polymers is studied theoretically and experimentally by considering local stretching of the molecular structure of a polymer by small-scale turbulent motions in the region very close to the wall. The stretching process is assumed to re-structure turbulence at small scales by forcing these to satisfy local axisymmetry with invariance under rotation about the axis aligned with the main flow. It is assumed that kinematic constraints imposed by local axisymmetry force turbulence near the wall to tend towards the one-component state and when turbulence reaches this limiting state it must be entirely suppressed across the viscous sublayer. These suggestions are supported by experiments which are carried out under well controlled laboratory conditions in a refractive index-matched pipe flow facility using laser-Doppler anemometry.

Introduction

Turbulent drag reduction due to the addition of small amounts of dilute polymers to flowing liquids has been known for more than 50 years. This phenomenon was discovered by Toms in 1948 and owing to his pioneering contribution it is often termed as Toms effect in the literature (Toms 1948). In spite of enormous research efforts in recent decades in attempts to provide at least a qualitative understanding of the chief mechanisms involved, no satisfactory explanation has yet been obtained. The problem of polymer drag reduction remains poorly understood mainly because the interaction between a polymer and turbulence is essentially at the molecular level of the former. This interaction involves modification of the molecular structure of a polymer by turbulent motions in the near-wall region. Fig. 1 shows a conceptual scenario where, under very special circumstances, turbulence in the near-wall region forces rolled-up chains of a polymer partially to unroll and stretch in the mean flow direction.

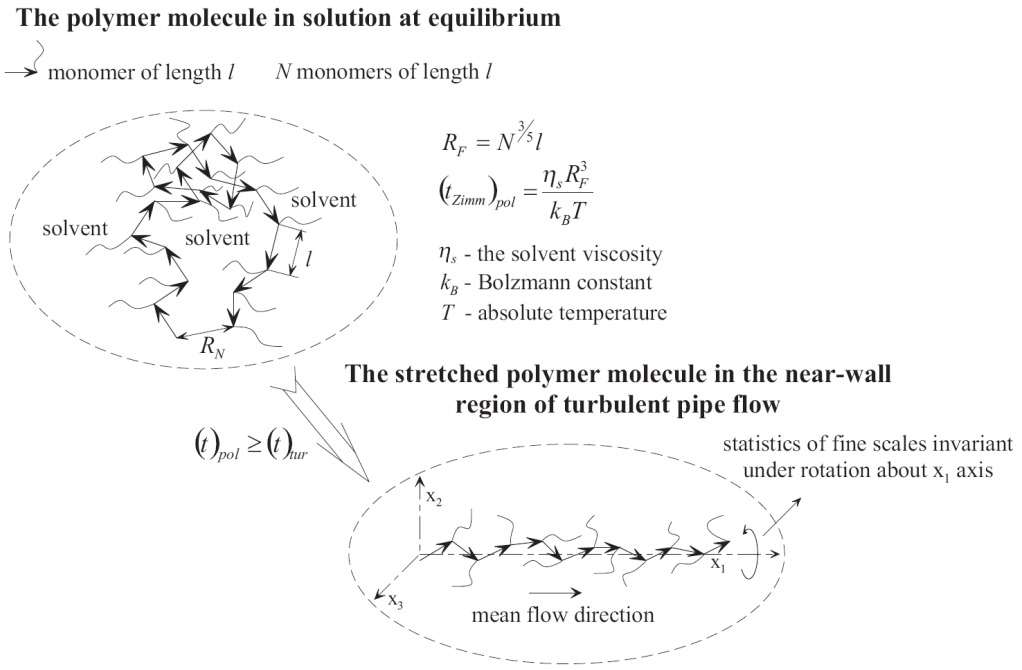

Fig. 1: Behavior of a polymer molecule in solution at equilibrium (top) and its response to stretching by turbulent motions at small scales very close to the wall (bottom).Here R_N and R_F are hydrodynamic and Flory radius, respectively.

In the unrolled state, polymer chains dictate characteristic length scales associated with the fine structure of turbulence. These scales are elongated in the streamwise direction and are therefore strongly anisotropic. In the most extreme case, polymer chains form a filament structure with a length-scale arrangement which is almost axisymmetric around the axis aligned with the mean flow. Hence it is reasonable to assume that the chief mechanism of drag reduction is related to the ability of the activated polymer to re-structure turbulence at small scales by forcing them to satisfy constraints imposed by local axisymmetry. Local axisymmetry as illustrated in Fig. 1 requires that the statistics of higher order velocity derivatives, which contribute to the turbulent dissipation correlations, must satisfy invariance under rotation about the axis orientated in the mean flow direction.

In the near-wall region, the presence of the polymer increases not only the anisotropy in length scales but also anisotropies in the dissipation and turbulent stresses, since these are closely related across the viscous sublayer. This can be shown using the two-point correlation technique and invariant theory (Jovanović 2004). If the polymer concentration (c) and its relaxation time (t_{pol}) are appropriately matched to the properties of turbulence, it will undergo considerable modification and reach, at the wall, a state of maximum anisotropy. This state can be identified on the anisotropy-invariant map shown in Fig. 2 and corresponds to the one-component limit ($II_a = 2/3$). For these limiting conditions Jovanović and Hillerbrand provided an analytical proof (see Jovanović et. al. 2005) which shows that if turbulence (at small scales) close to the wall is locally axisymmetric as illustrated in Fig. 1, it must undergo very rapid laminarization and therefore considerable drag reduction owing to suppression of the turbulent dissipation rate ε, which, under common circumstances, reaches a maximum at the wall.

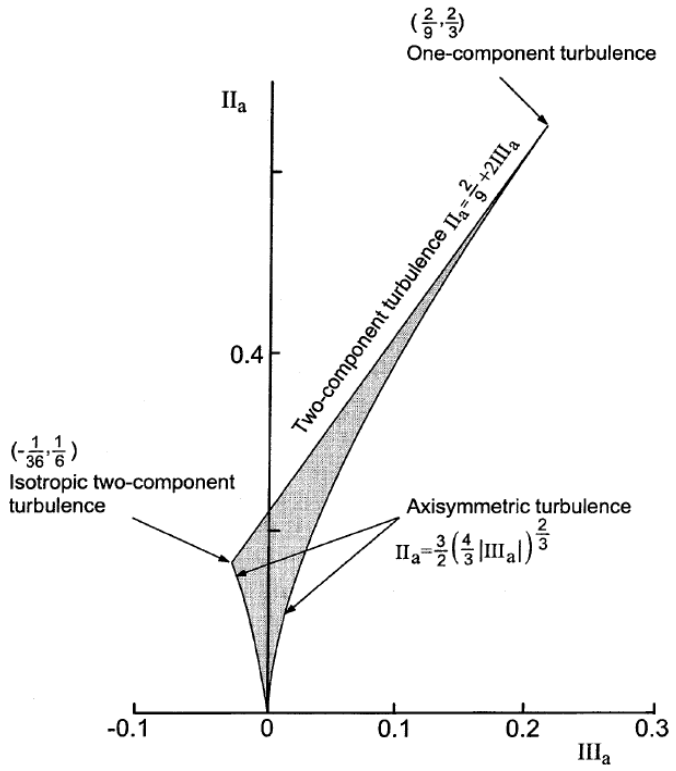

Fig. 2: Anisotropy-invariant map of the tensor $a_{ij}= \overline{u_i u_j}/q^2$-1/3 δ_{ij} and the limiting values of scalar invariants $II_a= a_{ij} a_{ji}$ $III_a= a_{ij} a_{jk} a_{ik}$ for the different states of the turbulence, after Lumley and Newmann 1977. Here, $\overline{u_i u_j}$ is the Reynolds stress tensor and q^2 is its trace expressed by $q^2= \overline{u_s u_s}$. According to Lumley 1978, all realistic turbulence must exist within the area delineated by the map.

Experimental verification of the chief mechanism of polymer drag reduction

In order to provide further experimental evidence that supports theoretical considerations of the chief mechanism responsible for polymer drag reduction, we decided to initiate an experimental program using laser-Doppler (LDA) measuring technique. This technique allows accurate experimental data to be obtained deep inside the viscous sublayer, enabling a quantitative basis to be formed for the interpretation of the dynamics of turbulence using the tools of invariant theory.

Measurements were performed in the refractive index-matched pipe-flow facility at the Institute of Fluid Mechanics in Erlangen. This test rig has been used extensively for different LDA measurements (siehe Durst et. al. 1995). It is a closed-loop pipe flow installation driven by a screw conveyor pump. Flow rates between 0.6 and 20 m^3 h^{-1} can be achieved with a tolerance of 1 %. With a pipe diameter of 50 mm a maximum Reynolds number of Re = $4.4x10^4$ can be realized. The test section is made of DURAN-50 glass. The flow was supplied from a large settling tank to the working section that was located about 4 m downstream, providing a development length of about 100 pipe diameters. In the present experiments, the flow was tripped at the pipe inlet to ensure additionally fully developed flow conditions. The test fluid (a mixture of two Diesel oils) was selected to match the refractive index of the glass. For simplification of the measurement and the traversing system, the pipe was mounted in a rectangular box (made of DURAN 50) through which the refractive index-matched fluid was also guided. Hence, the displacement of the LDA measuring control volume was directly proportional to the traversing performed.

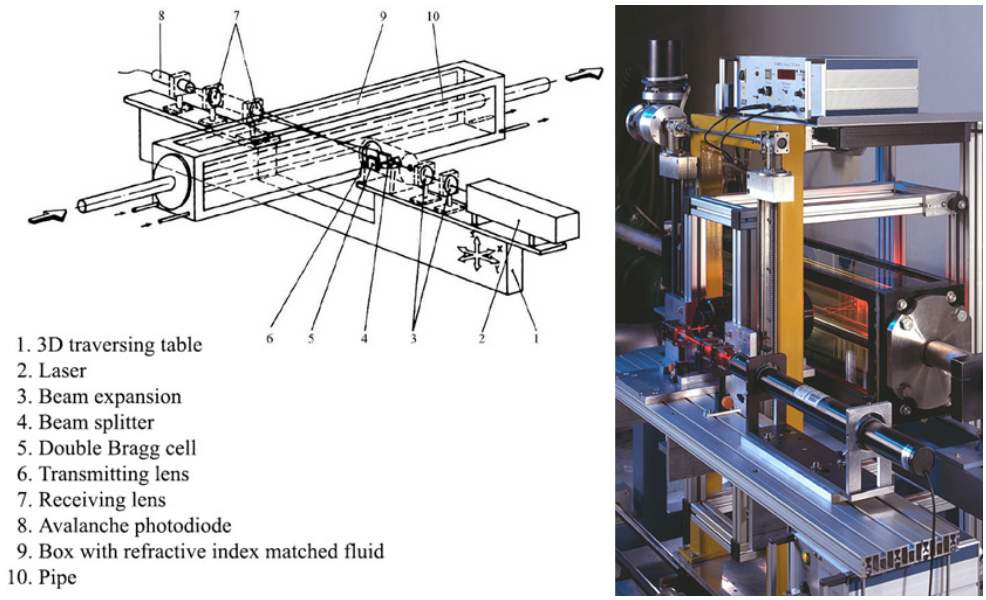

Fig. 3: Schematic and photographic views of the LDA System and the test section

The LDA measuring system was mounted on a 3-D traversing table, which could be moved in the plane normal to the pipe axis by using computer-controlled stepping motors and along the pipe axis with the help of a manual traversing system (see Fig. 3). The positions were read by digital indicators. The optical system consisted of a 15 mW helium-neon laser and a double Bragg cell unit. For measurements in the region away from the wall Bragg cells were driven at 40.0 and 41.5 MHz, providing a shift frequency of 1.5 MHz. In the near-wall region measurements were performed with the Bragg cells operated at 40.0 and 40.3 MHz, providing a shift frequency of 300 kHz. The measuring control volume was about 60 µm in diameter (minor axis d_2) and had a length of 230 µm (major axis d_1).

The LDA system employed was operated in the forward scattering mode. The image of the measuring volume was directed onto a pinhole in front of an Avalanche photodiode. In order to minimize the influence of noise on the measured data, the output signal from this diode was bandpass filtered before being processed by a TSI Model 1990 counter.

Although a fully developed state of turbulence at the measuring station had to be ensured, the facility was not operated at maximum speed, because the thickness of the viscous sublayer decreased with increasing mean flow velocity. To allow measurements in the direct proximity of the wall, a Reynolds number of 2.5×10^4 was chosen.

To quantify drag reduction, which is defined as

$$DR = 1 - \frac{\tau_{w,pol}}{\tau_w}, \tag{1}$$

it was necessary to determine the wall shear stress τ_w. This was accomplished by measuring the mean velocity at a fixed and predetermined position from the wall which was always within the viscous sublayer.

In order to analyse the structure of turbulence in a drag reduced flow using invariant theory, the second-order moments are required. For measurements in the viscous sublayer ($x_2^+ < 5$) it is possible to plot data in the anisotropy invariant map using axial and tangential fluctuation

values only. Fig. 4 shows DNS results (see Mansour et al. 1998) for x_2^+ < 5 plotted in the anisotropy invariant map: once using all Reynolds stress components and once using the $\overline{u_1^2}$ and $\overline{u_3^2}$ components only. It can be seen that there is no significant difference in the values obtained. Therefore, the mean velocity and the fluctuating components $\overline{u_1^2}$ in axial and $\overline{u_3^2}$ in tangential direction at a fixed position inside the region of the viscous sublayer were sufficient for the purpose of this investigation.

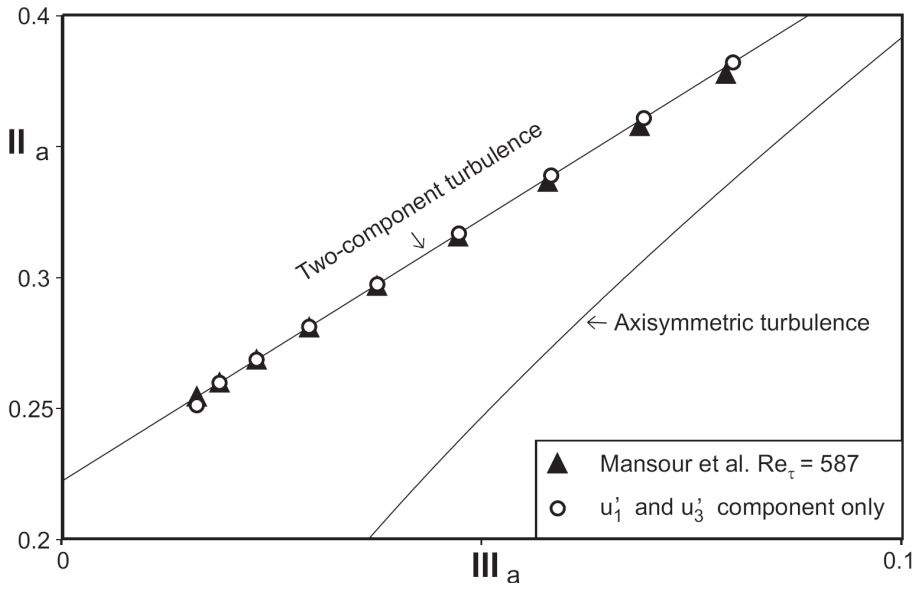

Fig. 4: DNS data (from Mansour et al. 1998) for x_2^+ < 5 plotted on the expanded scale in the anisotropy invariant map.

Experimental results

The polymer can be added to the flow in different ways. It can be injected into the flow at different concentrations or a homogeneous mixture can be prepared in advance. In order to guarantee a homogeneous mixture from the start it was decided to prepare the mixture outside the installation. A 50 ppm solution of a FORTUM polymer (see Fig. 5) was prepared by mixing it into oil. This mixture was stirred slowly for 1 week before distributing it to four 200 l kegs of Diesel oil yielding 5 and 10 ppm solutions, respectively. These solutions were stirred for another 24 h before being returned to the installation. Since the polymer is sensitive to mechanical straining, all these steps were performed very carefully and slowly. The viscosity was measured for the pure mixture of the two Diesel oils and the 50 ppm solution, yielding a constant kinematic viscosity of ν = 3.2x10^{-6} m s^{-2}.

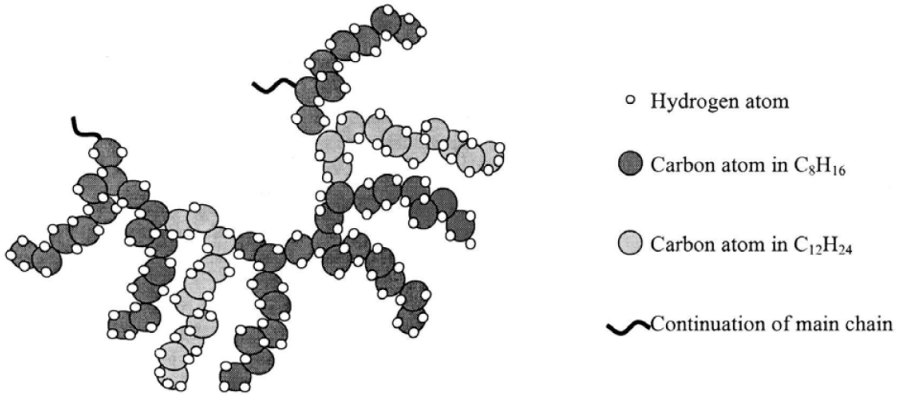

Fig. 5: Illustration of the molecular structure of a FORTUM polymer sample: $M \approx 25x10^6$ g mol^{-1}, $M_{dodecane}$ = 168.4320 g mol^{-1}, M_{octane} = 112.2880 g mol^{-1}, l = 2x1.54 Å, $r_{d/o} = C_{12}H_{24} / C_8H_{16}$ = 1/3, $N_{monomer} = M_{polymer} / [r_{d/o} M_{octane} + (1-r_{d/o}) M_{dodecane}]$

Since the polymer solution showed a rather short lifetime, with detectable degradation effects after 1 h of continuous operation, it was not possible to obtain the entire velocity profile of the flow in one session of measurements. Owing to the elaborate preparation procedure of the polymer solutions, the measurement of the entire velocity profile was abandoned and measurements at one point inside of the viscous sublayer were taken until the polymer had degraded and no further drag reduction could be observed. At regular time intervals, a sample of a working fluid was taken in order to check its kinematic viscosity, which was found to maintain a constant value.

Mean velocity and turbulence intensities in axial and tangential directions were measured for each of the solutions. Measurements were taken for about 10 h. Subsequently, the exact location of the measurement control volume was verified.

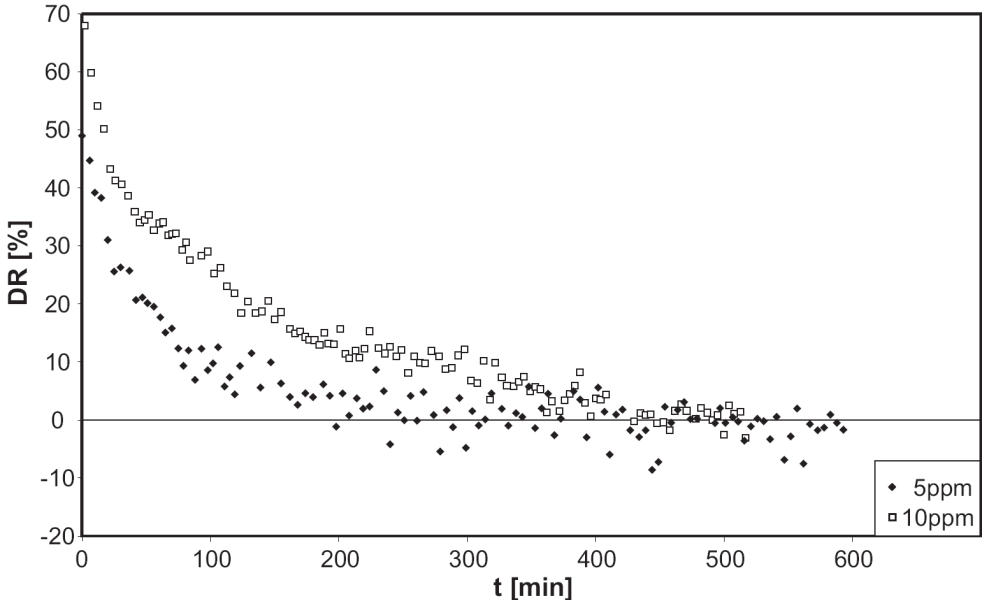

Fig. 6: Drag reduction for different concentrations of a polymer

As shown in Fig. 6, drag reduction decreased fast within the first 2 h. With an addition of 10 ppm polymers a maximum drag reduction of 70 % could be observed. The effect had completely vanished after continuous operation for 7.5 h. The highest value of drag reduction

with a 5 ppm polymer concentration was around 50 %. For this concentration of a polymer, the effect had disappeared 4 h after the beginning of the measurements.

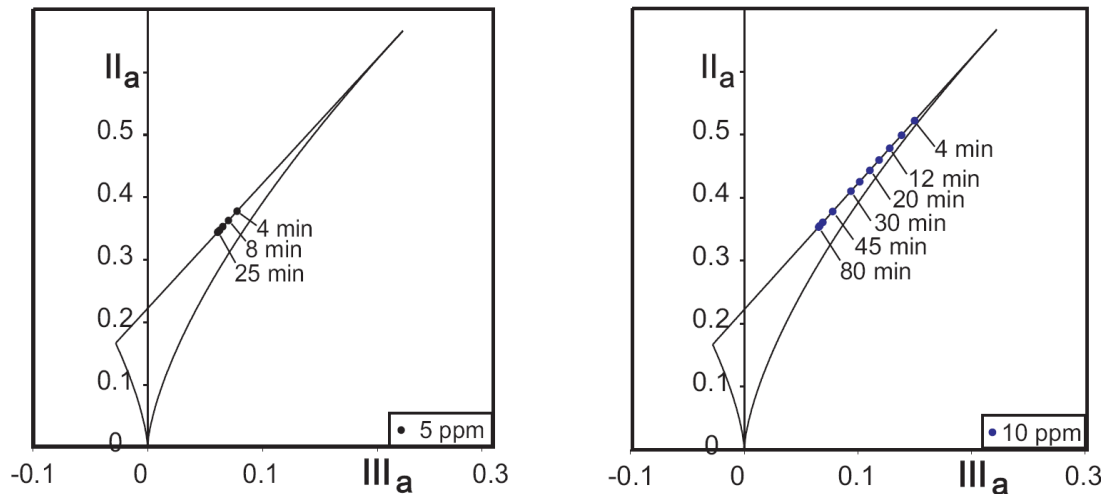

Fig. 7: Measurement results plotted on the anisotropy invariant map (together with those shown in previous figure) demonstrate that with decreasing DR the data points move away from the one-component limit.

The measured data were analysed by plotting these on the anisotropy invariant map. Fig. 7 shows the obtained results. The position of the initial point in the anisotropy invariant map depends on the polymer concentration and induced DR. With higher concentrations of a polymer its location moves closer to the one-component limit. The same trend can be observed in Newtonian fluids for decreasing Reynolds numbers (see Jovanović et. al. 2005). As time passes, the data indicate a clear tendency to move downwards along the two-component state line from a position close to the one-component limit towards a position close to the isotropic two-component limit. These results are in close agreement with those obtained from direct numerical simulations (Mansour et. el. 1998). The polymer degrades with time and the flow returns to its Newtonian behavior. The above-discussed trends in the anisotropy invariant map, which are associated with changes along the two-component state, for polymer concentrations of 5 and 10 ppm lasted about 25 and 80 min, respectively, before the trend in the data reversed direction on the anisotropy map. The reversed trend in the data corresponds roughly to a remaining drag reduction of about 30 %.

This reversed trend has no physical explanation but is caused by a reduced resolution in measurements due to the degradation of the polymer. Owing to polymer addition, the wall shear velocity u_τ decreased drastically. Thus, the initial dimensionless size of the measuring control volume was calculated to be

$$d_1^+ = 1 - \frac{d_1 u_{\tau,initial}}{\nu} \approx 3.2\,, \tag{2}$$

so that precise measurements in the viscous sublayer with $x_2^+ < 5$ were possible. With degradation of the polymer u_τ increased and also the dimensionless size of the measured control volume. At the point of 30 % drag reduction, the major axis d_1^+ assumed a value larger than the thickness of the viscous sublayer. For this reason, measurements in the viscous sublayer did not yield correct results for a low percentage of DR.

Conclusions

High spatial resolution laser-Doppler measurements were performed in a refractive index-matched pipe flow facility in order to provide experimental evidence that supports fundamentals associated with the chief mechanism responsible for polymer drag reduction. Special care was taken to maintain well-controlled flow conditions during the experiments and to account for all possible interferences that can influence the interpretation of the measured LDA signals. The experimental results for the mean velocity and turbulence intensity components obtained deep in the viscous sublayer permitted the evolution of turbulence to be traced across the anisotropy invariant map. Anisotropy invariant mapping of turbulence in the viscous sublayer reveals that with decrease of DR the anisotropy near the wall decreases along the line which characterizes the two-component state starting from nearly the one-component limit which correspond to large DR and finishing approximately midway between the one-component limit and the isotropic two-component limit for vanishing DR effect. These observations, extracted from the experimental results, are in close agreement with the theoretical analysis and support the notion that turbulent drag reduction by dilute addition of high polymers is associated with the ability of long-chain polymers to induce an increase in the anisotropy of turbulence in close proximity to the wall.

Acknowledgements

The authors gratefully acknowledge funding of the Erlangen Graduate School in Advanced Optical Technologies (SAOT) by the German Research Foundation (DFG) in the framework of the German excellence initiative.

References

Toms, B. A., 1948: “Some observations on the flow of linear polymer solutions through straight tubes at large Reynolds number”, Proc. 1st Intern. Cong. Rheol.

Jovanović, J., 2004: “The Statistical Dynamics of Turbulence”, Springer-Verlag, Berlin-Heidelberg

Lumley, J.L., Newman, G. 1977: “The return to isotropy of homogeneous turbulence”, J. Fluid Mech. Vol. 82, pp. 161-178

Lumley, J.L., 1978: ”Computational modeling of turbulent flows”, Adv. Appl. Mech., Vol. 18, pp. 123-176

Jovanović, J. and Hillerbrand, R., 2005: “On peculiar properties of the velocity fluctuations in wall-bounded flows”. Therm. Sci., Vol. 9, 3-12

Durst, F., Jovanović, J. and Sender, J., 1995: “LDA measurements in the near-wall region of a turbulent pipe flow”, J. Fluid Mech., Vol. 295, 305-335

Mansour, N.N., Moser, R.D. and Kim, J., 1998: “Fully developed turbulent channel flow simulations”, In AGARD Advisory Report 345, pp. 119-121